*Biochemical Journal* (2020) **477** 2039–2054
https://doi.org/10.1042/BCJ20200290

PORTLAND PRESS

Research Article

# Rationally designed peptide-based inhibitor of $A\beta_{42}$ fibril formation and toxicity: a potential therapeutic strategy for Alzheimer's disease

John R. Horsley[1,*], Blagojce Jovcevski[2,*], Kate L. Wegener[3], Jingxian Yu[1], Tara L. Pukala[2] and Andrew D. Abell[1]

[1]ARC Centre of Excellence for Nanoscale BioPhotonics (CNBP), Department of Chemistry, School of Physical Sciences, University of Adelaide, South Australia 5005; [2]Adelaide Proteomics Centre, Department of Chemistry, School of Physical Sciences, University of Adelaide, South Australia 5005; [3]School of Biological Sciences, University of Adelaide, South Australia 5005

**Correspondence:** John R. Horsley (john.horsley@adelaide.edu.au)



Amyloid beta peptide ($A\beta_{42}$) aggregation in the brain is thought to be responsible for the onset of Alzheimer's disease, an insidious condition without an effective treatment or cure. Hence, a strategy to prevent aggregation and subsequent toxicity is crucial. Bio-inspired peptide-based molecules are ideal candidates for the inhibition of $A\beta_{42}$ aggregation, and are currently deemed to be a promising option for drug design. In this study, a hexapeptide containing a self-recognition component unique to $A\beta_{42}$ was designed to mimic the β-strand hydrophobic core region of the Aβ peptide. The peptide is comprised exclusively of D-amino acids to enhance specificity towards $A\beta_{42}$, in conjunction with a C-terminal disruption element to block the recruitment of $A\beta_{42}$ monomers on to fibrils. The peptide was rationally designed to exploit the synergy between the recognition and disruption components, and incorporates features such as hydrophobicity, β-sheet propensity, and charge, that all play a critical role in the aggregation process. Fluorescence assays, native ion-mobility mass spectrometry (IM-MS) and cell viability assays were used to demonstrate that the peptide interacts with $A\beta_{42}$ monomers and oligomers with high specificity, leading to almost complete inhibition of fibril formation, with essentially no cytotoxic effects. These data define the peptide-based inhibitor as a potentially potent anti-amyloid drug candidate for this hitherto incurable disease.

## Introduction

Alzheimer's disease (AD) is the most common form of neurodegenerative disorder amongst the elderly, [1] leading to neuronal cell death and loss of cognitive function. It is the most prevalent neurodegenerative disease without a known cure, [2,3] with current drugs providing only marginal symptomatic relief. [4,5] While the exact cause of AD remains unclear, the major pathological hallmarks are neurofibrillary tangles and amyloid plaques in the brain. [6] Extracellular amyloid plaques are dense, insoluble aggregates containing the Aβ peptide, which in the brain are produced primarily by neurons. [7] Aβ is a short peptide, with the most common alloforms being either 40 or 42 residues in length, [8] and is formed via proteolysis of the amyloid precursor protein (APP) by β- and γ-secretases. [9,10] While $A\beta_{40}$ is the more abundant amyloid peptide *in vivo*, $A\beta_{42}$ is more neurotoxic and is responsible for peptide aggregation and fibrilization. [11] The aggregation of $A\beta_{42}$ peptide monomers to potentially neurotoxic oligomers and fibrils is believed to be a cause of AD, [12,13] however the precise relationship between size, structure and toxicity of $A\beta_{42}$ oligomers remains elusive. [14,15] The soluble monomeric form of $A\beta_{42}$ has recently been found to have possible additional physiological functions, [16] so the pursuit of drugs such as secretase inhibitors may not be prudent at this point in time. Hence, the inhibition of Aβ aggregation seems a more appropriate

*These authors contributed equally to this work.

Received: 14 April 2020
Revised: 12 May 2020
Accepted: 18 May 2020

Accepted Manuscript online: 19 May 2020
Version of Record published: 10 June 2020

Biochemical Journal (2020) 477 2039–2054
https://doi.org/10.1042/BCJ20200290

strategy.[17] The design of small molecular inhibitors to interfere with such protein-protein interactions is somewhat challenging, with the majority of those compounds currently undergoing clinical trials being non-selective and binding to $A\beta_{42}$ with low affinity. [12] Peptide-based molecules are ideal candidates for the inhibition of Aβ aggregation, insofar as they can be specifically modified to increase affinity and specificity, [12] with bio-inspired peptides currently considered to be the most promising option for drug design. [18–20] A rational approach for the design of peptide-based inhibitors expressly for $A\beta_{42}$ aggregation is to target the site where fibrilization is thought to occur, focusing on high specificity and affinity. [12] One of the sites known to be responsible for Aβ fibril formation is the hydrophobic core region of $A\beta_{42}$, the self-recognition 'nucleation site', KLVFF (16–20 residue region). [21,22] A synthetic peptide fragment comprising this amino acid sequence is believed to bind to the corresponding region of the native peptide via hydrophobic interactions and hydrogen bonding, providing minor inhibition of $A\beta_{42}$ aggregation. [23]

Studies have shown that $A\beta_{42}$ oligomers and fibrils contain a β-sheet structure, with the KLVFF region crucial in this regard. [24–28] It has been suggested that a conformational change to a β-sheet geometry is the first step in the aggregation process. [29] Recently, cryogenic electron microscopy (cryo-EM) and solid-state nuclear magnetic resonance (ssNMR) have revealed a detailed characterization of $A\beta_{42}$ monomers within the fibrils with near-atomic resolution. [30–32] These particular studies reveal that each amyloid polymorph results from the dimerization of two individual $A\beta_{42}$ molecules, with the stacking of identical monomer pairs above and below via hydrogen bonding to form oligomers. [33] In each of these defined polymorphs, a β-strand (16–20) region is evident in both monomers, with residues exposed on the exterior surface, forming the main turn between three major β-strands. These intramolecular β-strands, together with other critical interactions, such as a salt bridge between K28 and A42, help constrain the monomer into a compact S (or LS)-shaped amyloid fold, [30,34] as depicted in Figure 1A. A slight protrusion is evident in the structure towards the end of this particular β-strand, in the vicinity of hydrophilic residues E22 and D23, where several mutations are associated with the onset of Alzheimer's disease, [35] which may provide some insights into the origins of $A\beta_{42}$ toxicity.

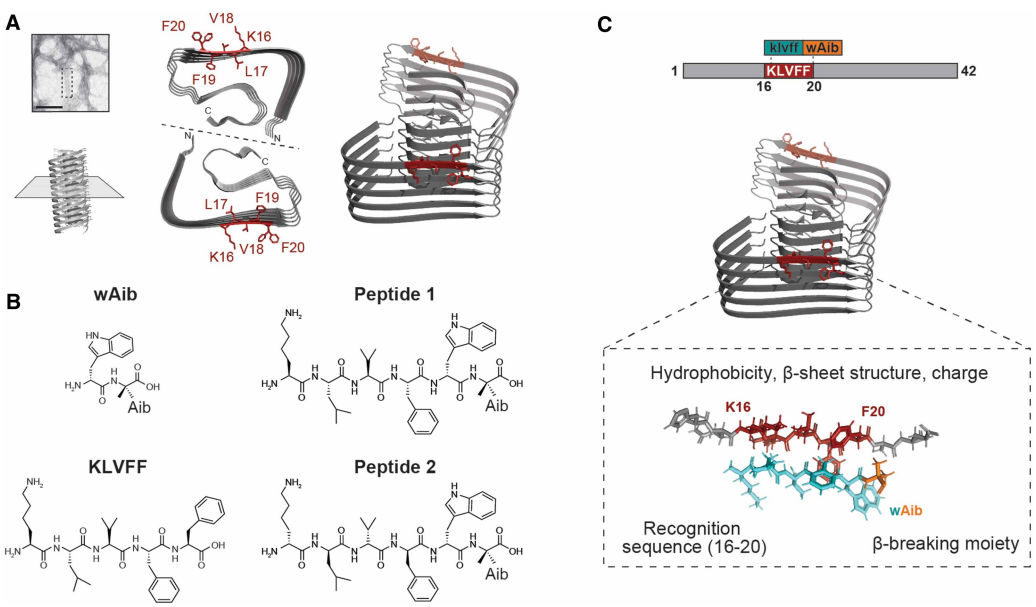


**Figure 1. High-resolution cryo-EM reconstruction of $A\beta_{42}$ fibrils, and synthesized peptides used in this study.**
(**A**) Cryo-EM reconstruction of full-length $A\beta_{42}$ fibrils (pdb entry: 5oqv) [32] shows that residues 16–20 (red) are central to a parallel β-sheet region, identified on the exterior surface of the fibrils in several $A\beta_{42}$ polymorphs. Residue F20 has been shown to occupy two distinct orientations on the fibril surface (fibril axis indicated by dashed line). (**B**) Structures of control peptides wAib and KLVFF. The rationally designed β-strand peptides **1** (L-isoform) and **2** (D-isoform) were assessed to determine their ability to prevent $A\beta_{42}$ fibril formation. (**C**) Design strategy of peptide inhibitors (peptide **2** in this instance) consisting of the recognition sequence (blue) which targets residues 16–20 (red) of $A\beta_{42}$, and the wAib β-breaker moiety (orange) to prevent fibril formation.

Biochemical Journal (2020) 477 2039–2054
https://doi.org/10.1042/BCJ20200290



Hence, these three-dimensional structures provide an excellent foundation for the rational design of inhibitors that can bind to a specific, accessible location on the monomer/fibril surface to prevent $A\beta_{42}$ aggregation.

Numerous derivatives of KLVFF have been developed to improve inhibitory effects, [36–42] with only pentapeptides or longer showing significant binding to the amyloid peptide. [43] A previous study based on the KLVFF motif, found that peptides containing D-amino acids were more active inhibitors of Aβ than their L-counterparts. [44] The D-amino acid peptide fragment, klvff, has a modest inhibitory effect on $A\beta_{42}$ aggregation, albeit superior to that of the L-enantiomer, KLVFF. [45] The use of D-amino acids offers advantages of increased metabolic stability and resistance to proteases, [46] decreased immunogenicity, [47] as well as an enhanced ability to cross the blood brain barrier (BBB). [48,49] Murphy and Kiessling were among the first to report incorporation of a 'disruption element' into peptides containing the KLVFF recognition element, which was shown to alter Aβ aggregation pathways. [50] Specifically, the recognition element facilitates the binding of the peptide-based inhibitor to the growing Aβ fibril or its precursor, while the disruption element is designed to hinder further propagation and reduce toxicity. [51,52] Peptides containing various 'β-strand breakers' acting as a disruption element have been shown to inhibit Aβ aggregation. [11,12] Proline residues were first used in this context, and exhibited a moderate inhibitory effect against $A\beta_{42}$ when located in the centre of the peptide sequence in order to prevent the formation of a β-sheet structure. [53] The achiral, geminally disubstituted aminobutyric acid (Aib) residue has also found moderate success when used in this manner, [2,54,55] and possesses a much stronger β-strand breaking potential than proline. [56] The placement of a β-strand breaker residue in the centre of short peptide inhibitors based on the KLVFF recognition element is known to distort the β-strand conformation, [57] and is thus not structurally homologous to the Aβ oligomer/fibril binding site. [52] The Gazit group designed a novel oligomerization inhibitor comprising a dipeptide, with D-tryptophan (D-Trp) coupled to a C-terminal Aib β-breakage moiety. [56] They found that tryptophan demonstrated the highest amyloidogenic propensity of any amino acid, [2] with the indole moiety thought to interact with the aromatic rings of the phenylalanine residues located in the central hydrophobic core region of the amyloid peptide via π–π stacking, thus competing with Aβ monomers for interaction with the growing fibrils. [56] While the peptide exhibited good binding affinity for Aβ monomers, [58] it was designed to be non-specific in sequence, and has the capacity to inhibit the toxic aggregation of other amyloid peptides, including IAPP, α-synuclein, and calcitonin. [59] Studies have shown that peptides with a high affinity for Aβ are better inhibitors of Aβ fibrilization, [60] but peptide-based inhibitors designed expressly for $A\beta_{42}$ aggregation also require high specificity. Hence, retention of the β-strand geometry of the peptide-based inhibitor for binding specificity is crucial, as is judicious placement of the disruption domain. Although a KLVFF fragment has been shown to inhibit $A\beta_{42}$ aggregation to a small degree, [23] it has a tendency to self-aggregate, which is not a desirable property for an effective inhibitor [61].

With the aforementioned in mind, we present a specific $A\beta_{42}$ inhibitor (see peptide **2** in Figure 1) based on the KLVFF recognition site of $A\beta_{42}$ (residues 16–20), that does not self-aggregate. The peptide comprises all D-amino acids, coupled to a C-terminal Aib 'β-breakage' moiety, to exploit the synergy between the recognition and disruption components. The peptide was rationally designed to incorporate features such as hydrophobicity, β-sheet propensity, and charge, in order to increase affinity and specificity, and provide a robust interconnection with $A\beta_{42}$, as all three elements play a critical role in the aggregation process. [46,62] Herein, we present structural studies of the peptide-based inhibitor and describe its effect on $A\beta_{42}$ aggregation and toxicity.

# Materials and methods

## Peptide synthesis

Peptides **1** and **2** were synthesized using Solid Phase Peptide Synthesis (SPPS). Fmoc-based SPPS and commercially available reagents were used for the synthesis of both peptides. 2-Chlorotrityl resin preloaded with Fmoc-Aib-OH (0.80 mmol $g^{-1}$, 1.0 g, 1 equiv) was used for both peptides. The unreacted active sites on the resin were capped with DCM/MeOH/DIPEA (17:2:1, 2 × 25 ml) for 30 min and the resin washed with DCM (x3), DMF (x3) and DCM (x3). *N*-Fmoc deprotection was conducted by treating the resin with 25% piperidine/DMF (25 ml) for 30 min before washing with DCM (x3), DMF (x3) and DCM (x3). Each sequential amino acid was coupled using the following molar ratios of reagents: Fmoc-amino acids were each dissolved in DMF (20 ml), 1-[bis(dimethylamino)methylene]-1*H*-1,2,3-triazolo[4,5-*b*]pyridinium 3-oxid hexafluorophosphate (HATU)/DMF (0.5 M, 2 equiv) and DIPEA (4 equiv). The resin was then washed with DCM (x3) and

Biochemical Journal (2020) 477 2039–2054
https://doi.org/10.1042/BCJ20200290

DMF (x3) followed by DCM (x3), and the coupling procedures repeated. The coupling time was a minimum of 2 h in all cases. Fmoc-(D)-Trp-OH was next added to each peptide. Thereafter, Fmoc-(L)-Phe-OH, Fmoc-(L)-Val-OH, Fmoc-(L)-Leu-OH, and Fmoc-(L)-Lys(Boc)-OH were sequentially added to peptide **1**, whereas all D-amino acids, Fmoc-(D)-Phe-OH, Fmoc-(D)-Val-OH, Fmoc-(D)-Leu-OH, and Fmoc-(D)-Lys (Boc)-OH were used to synthesize peptide **2**. Following coupling with the final residue for each peptide, treatment with 1.5% TFA/DCM (15 ml) for 10 min resulted in cleavage from the resin. Peptides **1** and **2** were each dissolved in TFA/DCM (50% v/v) for 30 min to remove the Boc protecting group. Each peptide was placed under vacuum before being purified using reverse phase HPLC. KLVFF and wAib-OH (controls) were also synthesized using SPPS, and purified using reverse phase HPLC. Notably, a number of techniques including $^1$H NMR, were used to confirm that peptides **1** and **2** have been stable for more than two years.

## $^1$H NMR data for peptides

Peptide **1** $^1$H NMR (600 MHz, DMSO-d6) δ 10.79 (s, 1H, OH), 8.47 (d, 1H, NH Leu, $J$ = 8.0 Hz), 8.30 (d, 1H, NH Trp, $J$ = 8.4 Hz), 8.13–8.10 (m, 3H, NH Aib, $NH_2$ terminal Lys), 7.93 (d, 1H, NH Val, $J$ = 9.0 Hz), 7.87 (d, 1H, NH Phe, $J$ = 7.7 Hz), 7.75 (br s, 1H, NH indole), 7.66 (d, 1H, ArH, $J$ = 7.9 Hz), 7.30 (d, 1H, ArH, $J$ = 8.1 Hz), 7.12 (d, 1H, ArH, $J$ = 2.1 Hz), 7.10–7.04 (m, 4H, ArH), 6.98 (t, 1H, ArH, $J$ = 7.5 Hz), 6.94 (d, 2H, ArH, $J$ = 7.1 Hz), 4.54–4.49 (m, 2H, CαH Phe, CαH Trp), 4.40 (m, 1H, CαH Leu), 4.08 (m, 1H, CαH Val), 3.76 (m, 1H, CαH Lys), 3.12 (m, 1H, CαH (Trp) C*H*H), 2.84 (m, 1H, CαH (Trp) CH*H*), 2.70 (m, 2H, CαH (Lys) $CH_2CH_2CH_2CH_2$), 2.65 (m, 1H, CαH (Phe) C*H*H), 2.51 (m, 1H, CαH (Phe) CH*H*), 1.88 (m, 1H, CαH (Val) C*H*), 1.68–1.62 (m, 2H, CαH (Lys) $CH_2CH_2CH_2CH_2$), 1.58 (m, 1H, CαH (Leu) $CH_2CH$), 1.51–1.46 (m, 2H, CαH (Lys) $CH_2CH_2CH_2CH_2$), 1.40–1.34 (m, 2H, CαH (Leu) $CH_2CH$), 1.37 (s, 3H, Aib $CH_3$), 1.32 (s, 3H, Aib $CH_3$), 1.30–1.27 (m, 2H, CαH (Lys) $CH_2CH_2CH_2CH_2$), 0.87–0.82 (m, 6H, (Leu) 2 × $CH_3$), 0.75–0.73 (m, 6H, (Val) 2 × $CH_3$).

HRMS $[M + H]^+$ calc'd = 777.4663, $[M + H]^+$ found = 777.4674 (Supplementary Figure S11).

Peptide **2** $^1$H NMR (600 MHz, DMSO-d6) δ 10.80 (s, 1H, OH), 8.47 (d, 1H, NH Leu, $J$ = 8.0 Hz), 8.07 (s, 1H, NH Aib), 8.05 (d, 1H, NH Trp, $J$ = 8.2 Hz), 7.99 (d, 1H, NH Val, $J$ = 9.1 Hz), 7.95 (d, 1H, NH Phe, $J$ = 8.1 Hz), 7.73 (br s, 1H, NH indole), 7.57 (d, 1H, ArH, $J$ = 7.9 Hz), 7.31 (d, 1H, ArH, $J$ = 8.1 Hz), 7.21–7.12 (m, 6H, ArH), 7.05 (t, 1H, ArH, $J$ = 7.1 Hz), 6.96 (d, 1H, ArH, $J$ = 7.0 Hz), 4.57–4.52 (m, 2H, CαH Phe, CαH Trp), 4.40 (m, 1H, CαH Leu), 4.11 (m, 1H, CαH Val), 3.76 (t, 1H, CαH Lys, $J$ = 6.2 Hz), 3.07 (m, 1H, CαH (Trp) C*H*H), 2.98–2.92 (m, 2H, CαH (Trp) CH*H*, CαH (Phe) C*H*H), 2.75 (m, 1H, CαH (Phe) CH*H*), 2.70 (m, 2H, CαH (Lys) $CH_2CH_2CH_2CH_2$), 1.88 (m, 1H, CαH (Val) C*H*), 1.69–1.63 (m, 2H, CαH (Lys) $CH_2CH_2CH_2CH_2$), 1.59 (m, 1H, CαH (Leu) $CH_2CH$), 1.52–1.46 (m, 2H, CαH (Lys) $CH_2CH_2CH_2CH_2$), 1.42 (m, 1H, CαH (Leu) C*H*HCH), 1.35 (m, 1H, CαH (Leu) CH*H*CH), 1.32 (s, 3H, Aib $CH_3$), 1.31–1.23 (m, 2H, CαH (Lys) $CH_2CH_2CH_2CH_2$), 1.27 (s, 3H, Aib $CH_3$), 0.88–0.83 (m, 6H, (Leu) 2 × $CH_3$), 0.74–0.72 (m, 6H, (Val) 2 × $CH_3$).

HRMS $[M + H]^+$ calc'd = 777.4663, $[M + H]^+$ found = 777.4706 (Supplementary Figure S12).

## IR spectroscopy

Infrared spectra of peptides **1** and **2** (dried samples) were collected on a PerkinElmer Spectrum 100 FT-IR spectrometer, with attenuated total reflectance (ATR) imaging capabilities, fitted with a ZnSe crystal, with an average reading taken from four scans at 4 $cm^{-1}$ resolution.

## High-performance liquid chromatography

The synthetic peptides were analyzed and purified by reverse phase HPLC, using a Gilson GX-271 preparative system equipped with Trilution LC 2.1 software, with a Supelco C18 column (250 × 10 mm) at a flow rate of 4 ml $min^{-1}$. ACN/TFA (100/0.0008 by v/v) and water/TFA (100/0.001 by v/v) solutions were used as organic and aqueous buffers, respectively.

## High resolution mass spectroscopy

High resolution mass spectral data were analyzed using an Ultimate 3000 RSL HPLC (Thermo Fisher Scientific Inc., MA) and an LTQ Orbitrap XL ETD using a flow injection method, with a flow rate of 5 µl/min. The HPLC flow is interfaced with the mass spectrometer using the Electrospray source (Thermo Fisher Scientific Inc., MA). Mass spectra were obtained over a range of $100 < m/z < 1000$. Data was analyzed using XCalibur software (Version 2.0.7, Thermo Fisher Scientific).

## Molecular modelling

The lowest-energy conformers for the peptides were determined in the gas phase by the NWChem 6.6 package [63] with tight convergence criteria using a hybrid B3LYP functional with 6–31G** basis set for all atoms. Conformational analysis, including dihedral angles, overall molecular lengths and intramolecular hydrogen bond lengths, were conducted using the Chimera 1.11software. [64]

## $A\beta_{42}$ aggregation assays

Monomerization of $A\beta_{42}$ (Adelab Scientific) was prepared by NaOH treatment as described previously [65] whereas mature $A\beta_{42}$ fibrils were prepared at 37°C for 24 h with shaking (50 rpm). The ability of various inhibitors to prevent $A\beta_{42}$ fibril formation was assessed using an *in situ* thioflavin-T (ThT) (20 μM) assay. Non-monomerized $A\beta_{42}$ (100 μM) was examined across a range of molar ratios (1 : 1, 1 : 2, 1 : 10 and 1 : 20) ($A\beta_{42}$:inhibitor) in the absence and presence of inhibitors. Assays were performed in PBS (pH 7.4) and 1% DMSO at 35°C in quiescence. The ability of the inhibitors to prevent $A\beta_{42}$ fibrilization was determined by comparing the ThT fluorescence at the conclusion of each assay. [66] The inhibition of primary-nucleation mediated $A\beta_{42}$ aggregation was also monitored using an *in situ* ThT assay where monomerized $A\beta_{42}$ (10 μM) was incubated in the absence and presence of inhibitors under conditions stated above at 25°C. All assays were performed using a FLUOstar Optima plate reader (BMG Lab Technologies) with excitation and emission wavelengths set at 440 nm and 490 nm, respectively. All assays were performed at least three times and data are reported as mean ± SEM of three independent assays.

## Seeded α-synuclein (αS) aggregation assays

Plasmid (pT7–7, Addgene) encoding for wild-type (WT) human αS (SNCA, UniProt accession number: P37840) were kindly donated by Prof. Heath Ecroyd (University of Wollongong, Australia). Expression and purification of monomeric αS WT was performed as described previously. [67] Following purification, monomeric αS (50 μM in PBS) was heated and stirred at 45°C for 24 h prior to sonication. The ability of peptides **1** and **2** to prevent αS fibril formation was assessed using an αS elongation assay. [67] This assay measures the ability of the designed inhibitors to inhibit the elongation of αS fibrils using short pre-formed αS seed fibrils. Elongation of αS fibrils was monitored using an *in situ* ThT (20 μM) assay. Inhibitors were added at 1 : 1, 2 : 1 and 1 : 2 molar ratios (αS:inhibitor) to monomeric αS (50 μM) in PBS (pH 7.4) with 5% (w/w) αS seed fibrils. All assays were performed at least three times and data are reported as mean ± SEM of these independent assays.

## TEM

The presence and morphology of $A\beta_{42}$ fibrils were imaged by TEM where 2 μl aliquots from the end-point of ThT aggregation assays were adsorbed on to carbon-coated electron microscopy grids (SPI Supplies) and negatively stained with 2% (w/v) uranyl acetate. [68] Images were viewed using a Philips CM100 transmission electron microscope at 45 000× magnification.

## Nile red assays

Nile red fluorescence was used to determine the relative amount of exposed hydrophobicity of $A\beta_{42}$ fibrils and measured using a Cary Eclipse fluorescence spectrophotometer (Varian). Fibrils (10 μM in PBS, pH 7.4) in the presence and absence of inhibitors were labelled with Nile red (10 μM). Labelled samples were incubated for 5 min at room temperature prior to fluorescence measurement. The excitation wavelength was set at 595 nm and emission wavelength was recorded from 500–800 nm. The slit widths for excitation and emission spectra were both set at 5 nm.

## Cell culture and cell viability assays

Mouse neuroblastoma Neuro-2a cells were kindly donated by Dr. David Bersten (University of Adelaide, Australia) and grown in DMEM/F12 media containing 10% fetal calf serum at 37°C in 5% $CO_2$/95% air atmosphere. Cells were seeded at $3 \times 10^4$ cells/well in aforementioned media and equilibrated for 24 h prior to addition of pre-formed $A\beta_{42}$ fibrils (50 μM) in the absence and presence of each inhibitor at a 1 : 2 ($A\beta_{42}$ : inhibitor) molar ratio. Cells were then incubated for 48 h at 37°C in 5% $CO_2$/95% air atmosphere prior to cell viability measurement. The ability of the inhibitors to prevent cytotoxicity induced by the addition of

Biochemical Journal (2020) 477 2039–2054
https://doi.org/10.1042/BCJ20200290

exogenous $A\beta_{42}$ fibrils was assessed using a thiazolyl blue tetrazolium bromide (MTT) assay. Media was removed post-incubation and replaced with serum-free media containing MTT (0.25 mg/ml) and incubated for 2 h at 37°C in 5% $CO_2$/95% air atmosphere. Media containing MTT was removed and cells were lysed with DMSO prior to absorbance measurement at 570 nm using a FLUOstar Optima plate reader (BMG Lab Technologies). Statistical analysis was performed using Prism 8.0 (GraphPad).

### Native ion mobility—mass spectrometry (IM-MS)

IM-MS was performed as described previously [68] on a Synapt G1 HDMS (Waters) with a nanoelectrospray source. $A\beta_{42}$ (10 μM) was incubated in the absence and presence of peptide 1/2 at a 1 : 10 molar ratio ($A\beta_{42}$ : peptide **1**/**2**) in 200 mM ammonium acetate (pH 6.8) and loaded onto platinum-coated borosilicate glass capillaries prepared in-house (Harvard Apparatus). To minimize gas-phase structural rearrangement the following instrument parameters were applied: capillary voltage, 1.65 kV; sample cone voltage, 20 V; source temperature, 25°C; trap collision energy, 10–20 V (5 V increments); transfer collision energy, 10 V; trap gas: 4.5 l/h; backing pressure, 4.0 mbar. IM cell instrument parameters: wave velocity: 300 m/s; transfer t-wave height: 6 V; transfer wave velocity: 250 m/s. Mass spectra and ATD data were analyzed using MassLynx (v4.1) and Driftscope (v2.7) respectively (Waters).

## Results and discussion

### Peptide design

Peptide **2** and its natural analogue **1** (Figure 1B) were designed specifically to inhibit the aggregation of $A\beta_{42}$. The peptide sequence is based on the hydrophobic core, KLVFF recognition region of $A\beta_{42}$, with the terminal phenylalanine residue of each replaced with D-Trp which is known to enhance amyloidogenicity, and with an appended C-terminal achiral Aib residue to act as a β-strand breaker. The peptides were designed to adopt a β-strand geometry and bind specifically to the KLVFF region of $A\beta_{42}$ by virtue of their sequence homology, with the Aib residue proposed to interfere with the aggregation process.

As previously demonstrated, [27] a peptide-based inhibitor containing a preorganized β-strand conformation, facilitates binding to early β-structured oligomers to a greater extent than unstructured monomers bind oligomers. With respect to oligomeric amyloid structures, it has been proposed that a parallel β-sheet forms between neighboring $A\beta_{42}$ monomers at the central 15–21 residue region. [40] An antiparallel β-sheet has also been suggested for the interaction between short inhibitory peptides containing D-amino acids and the all L-$A\beta_{42}$, generating energetically favourable hydrogen bonding. [52] The C-terminal Aib residue is intended to sterically block hydrogen bonding between the β-sheets in either orientation, while also increasing the overall hydrophobicity of the peptide. An Aib moiety is known to promote helicity which then disrupts β-sheet formation, leading to inhibition of amyloid formation. [55] The mass of the peptide was restricted to 776 Da, without compromising functionality, since compounds with a mass in excess of 1000 Da are largely excluded from passing through the BBB. [69] Peptide fragments, KLVFF and D-Trp-Aib-OH (hereafter referred to as wAib, Figure 1B) were used as controls for the aggregation studies, as peptides **1** and **2** were both derived from the KLVFF region of $A\beta_{42}$, and each contain an Aib residue coupled to a D-Trp at their C-termini.

### Conformational analysis of peptides

The backbones of peptides **1** and **2** were shown to adopt a β-strand geometry by $^1$H NMR, IR and molecular modelling. Specifically, CαH (*i*) to NH (*i* + 1) and $C\beta H_2$ (*i*) to NH (*i* + 1) ROESY interactions for residues 1–5 were observed (excluding Aib, see Supplementary Figures S1, S2). Four $^3J_{NHC\alpha H}$ coupling constants between 7.7 Hz and 9.0 Hz were observed for peptide **1**, while $^3J_{NHC\alpha H}$ coupling constants between 8.0 Hz and 9.1 Hz were observed for residues 2–5 in peptide **2** (excluding Aib), in accordance with a β-strand conformation. [70] The IR spectrum of peptide **1** shows a strong Amide I band at 1637 $cm^{-1}$, characteristic of a β-strand conformation, together with an Amide II band at 1550 $cm^{-1}$ (N-H bending vibrations, parallel β-sheet), [71] and Amide A band at 3275 $cm^{-1}$ (N-H stretching, Supplementary Figure S3). The IR spectrum for peptide **2** is also characteristic of a β-strand conformation, with a strong Amide I band at 1631 $cm^{-1}$, and an Amide II band at 1525 $cm^{-1}$, indicative of an antiparallel β-sheet (Supplementary Figure S4). [71] The lowest energy conformer for the D-peptide **2** was determined by density functional theory (DFT) calculations to further define the backbone geometry (see Materials and Methods section for details). The backbone dihedral angles for **2** indicate a β-strand geometry throughout the peptide, from D-Lys (1) to D-Trp (5), with the exception of the Aib residue

(Supplementary Table S1). This result supports the IR and $^1$H NMR spectroscopic data, which also confirms an extended β-strand conformation, with the exception of the C-terminal Aib 'β-breaker' moiety. Furthermore, critical distances calculated for CαH (*i*) to NH (*i* + 1) and CβH$_2$ (*i*) to NH (*i* + 1) are in accordance with a β-strand conformation (Supplementary Figures S5–S7 and Supplementary Table S2). [72]

## Peptide 2 significantly inhibits Aβ$_{42}$ fibril elongation

Peptides **1** and **2** were each tested for inhibition of Aβ$_{42}$ elongation, with control peptides KLVFF and wAib used for comparison. The ability of the peptides to inhibit Aβ$_{42}$ aggregation was assessed using an *in vitro* thioflavin-T (ThT) fluorescence assay (see Materials and Methods section for details), which exhibits increased fluorescence with the extent of cross β-sheet structure, characteristic of amyloid fibril formation. [38] In the absence of inhibitors, Aβ$_{42}$ follows aggregation kinetics whereby fibril elongation begins immediately (i.e. seeding-like kinetics), reaching a plateau at ∼6 h (Figure 2A) likely due to the high concentration of Aβ$_{42}$ (100 μM) as observed previously [73]. In the presence of wAib, no drastic change in ThT fluorescence was observed over time, until a 20-fold excess led to an observable decrease in fluorescence (Figure 2A; dark grey). In the presence of KLVFF, small decreases in fluorescence were observed at 2-fold and 10-fold excess compared with Aβ$_{42}$ alone (Figure 2A; light grey). Conversely, in the presence of either peptides **1** or **2**, a dramatic decrease in fluorescence was observed compared with Aβ$_{42}$ alone (Figure 2A; dark and light blue, respectively). Essentially, peptide **2** achieved near complete inhibition at a 1 : 2 molar ratio (Figure 2A,B).

The specificity of each peptide to Aβ$_{42}$ was also assessed by performing an α-synuclein (αS) fibril elongation assay and measuring the change in ThT fluorescence. An abnormal accumulation of α-synuclein protein in the brain is associated with the onset of Parkinson's disease. [74] In the presence of these inhibitors, only peptide **1** displayed a distinct decrease in fluorescence at a 1 : 2 molar ratio (αS:inhibitor) (Supplementary Figure S10). Notably, peptide **2** showed no effect on α-synuclein aggregation, demonstrating the significance of the specific D-amino acid sequence, and the secondary structure within this potent peptide-based inhibitor for specificity towards Aβ$_{42}$.

Transmission electron microscopy (TEM) was also used to examine the morphology of Aβ$_{42}$ fibrils in the absence and presence of the inhibitory peptides at the conclusion of the aggregation assays. In the absence of inhibitors, Aβ$_{42}$ incubated alone is observed to form a dense network typical of amyloid fibrils (Figure 2C). In the presence of either wAib or KLVFF, Aβ$_{42}$ also exhibits a dense fibrillar structure at the molar ratio tested (1 : 2) (Aβ$_{42}$:inhibitor) (Figure 2C). Previous studies, using a KLVFF-NH$_2$ peptide as a control, observed similar dense fibrilization when incubated with Aβ$_{42}$ at a similar stoichiometric ratio. [37,42] In the presence of peptide **1**, the abundance of Aβ$_{42}$ fibrils is reduced considerably when compared with the two controls (Figure 2C). However, in the presence of peptide **2**, small fibril seeds are sparsely distributed, with no large fibrillar structures observed (Figure 2C), highlighting its capacity as a potent inhibitor. Overall, the data from the ThT assays are commensurate with the associated TEM images for both controls and peptide inhibitors.

Due to the absence of an observable lag-phase where primary nucleation would occur, changes in ThT fluorescence during the elongation phase (Figure 1A, 0.5–2.5 h) were examined to determine the elongation rate from the range of molar ratios tested (Figure 3A and Supplementary Table S3). Both wAib and KLVFF do not drastically affect the rate of Aβ$_{42}$ fibril elongation (Figure 3A and Supplementary Table S3). In contrast, peptides **1** and **2** significantly reduce the rate of fibril elongation such that a 10-fold excess of peptide **2** remarkably halts fibril elongation altogether (Figure 3A and Supplementary Table S3). In addition, the relationship between inhibitor concentration and Aβ$_{42}$ was determined to provide evidence as to whether peptides **1** and **2** interact with Aβ$_{42}$ species to attenuate fibril formation (Figure 3B). As the concentration of wAib and KLVFF increases there is little effect on fibril elongation (i.e. less than a 50% decrease in the elongation rate at a 20-fold excess). However, as the concentration of peptides **1** and **2** increases there is a dramatic reduction in fibril elongation, suggesting that these peptides interact with fibrillar Aβ$_{42}$ and prevent further monomer recruitment.

In addition, the mechanism(s) in which peptides **1** and **2** prevent Aβ$_{42}$ fibrilization were probed by examining their ability to disassemble pre-formed fibrils (Figure 3C). Fibril elongation was allowed to proceed for 4.5 h, at which point a 10-fold molar excess of either peptide **1** or **2** was added (Figure 3C, red dashed line). In contrast with peptide **1**, peptide **2** exhibits a plateau in ThT fluorescence for the duration of the assay (Figure 3C). Collectively, this indicates that the peptides, particularly **2**, do not disassemble pre-formed fibrils but interact with the ends of fibrils to prevent subsequent elongation. Overall the data indicates that both peptides, in particular peptide **2**, preferentially interact with Aβ$_{42}$ fibrils to prevent further fibrilization. The fact

Biochemical Journal (2020) 477 2039–2054
https://doi.org/10.1042/BCJ20200290

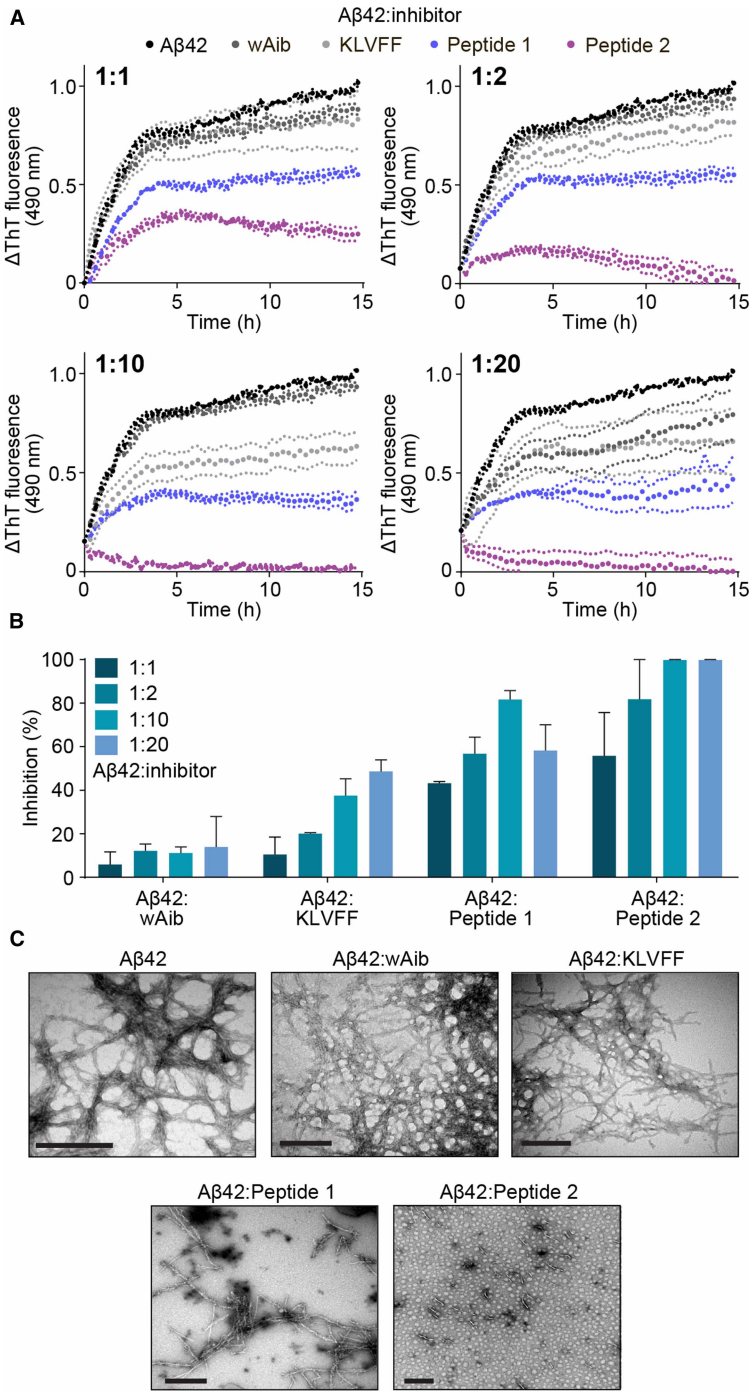


**Figure 2. Peptide 2 as a most effective inhibitor of $A\beta_{42}$ fibril elongation.**

(**A**) ThT fluorescence assay monitoring fibril elongation and formation of $A\beta_{42}$ in the absence (100 μM, black) and presence of wAib (dark grey), KLVFF (light grey) and peptide inhibitors **1** (blue) and **2** (purple) at various molar ratios (ranging from 1 : 1 to 1 : 20 $A\beta_{42}$ : inhibitor). (**B**) The degree of inhibition of $A\beta_{42}$ fibril elongation (calculated at the conclusion of the assay) of wAib, KLVFF, **1** and **2** across the range of molar ratios. Data reported in A and B is presented as mean ± SEM ($n = 3$). (**C**) TEM images of mature $A\beta_{42}$ fibrils in the absence and presence of inhibitors at a 1 : 2 molar ratio ($A\beta_{42}$ : inhibitor). Scale bars represent 200 nm.

*Biochemical Journal* (2020) **477** 2039–2054
https://doi.org/10.1042/BCJ20200290

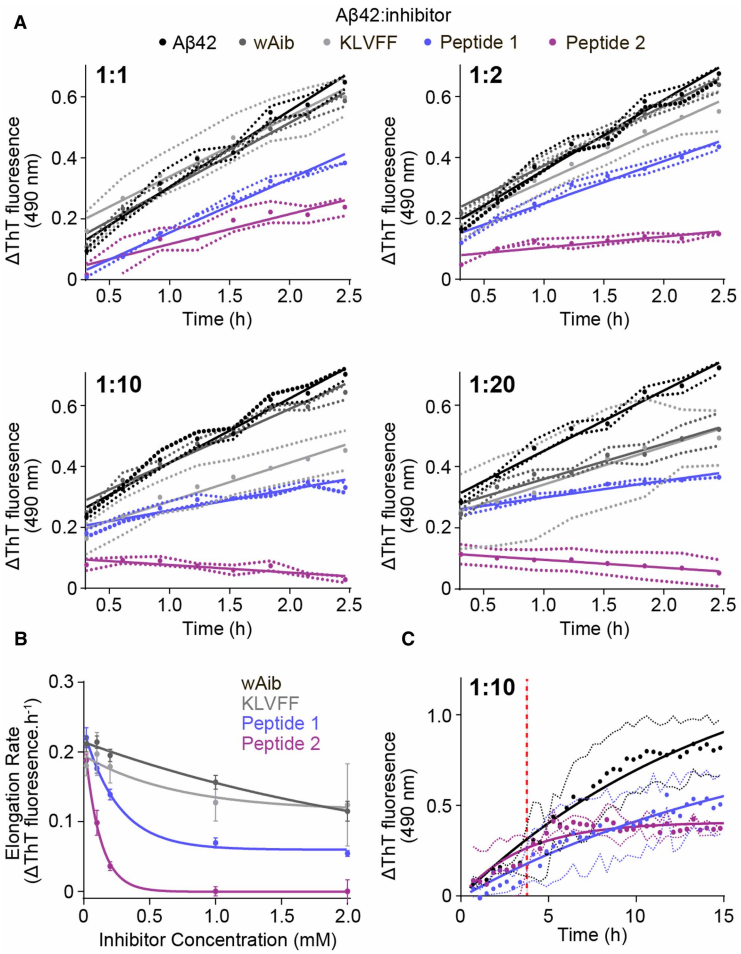


**Figure 3. Peptide 2 drastically reduces the rate of $A\beta_{42}$ fibril elongation.**

(**A**) The change in ThT fluorescence during the elongation phase of $A\beta_{42}$ (100 μM) fibril formation in the absence (black) and presence (grey, blue and purple) of inhibitors at a range of molar ratios (0–2.5 h from Figure 2A). (**B**) The rate of $A\beta_{42}$ fibril elongation as a function of inhibitor concentration (mM) was fitted with a non-linear one-phase decay fit. (**C**) ThT fluorescence assay of $A\beta_{42}$ (10 μM) spiked after 4.5 h (red dashed line) with peptides **1** and **2** (100 μM) during incubation where no decrease in fibrilization was observed. Data reported is presented as mean ± SEM ($n = 3$).

that peptide **2** does not disassemble existing fibrils, thereby potentially avoiding the formation of toxic oligomers, reinforces the feasibility of the proposed binding mode (mechanism) where a robust interconnection is made between the two by virtue of their sequence homology, heterochiral nature, and complementary β-strand conformation.

## Peptide 2 also interacts with $A\beta_{42}$ monomers by inhibiting primary nucleation mediated $A\beta_{42}$ fibril formation

The ability of peptides **1** and **2** to prevent primary nucleation mediated $A\beta_{42}$ fibril formation was also assessed by ThT fluorescence assays. Under conditions that induce primary nucleation fibril formation (typically 5–10 μM)[65,75] and in the absence of inhibitors, $A\beta_{42}$ follows sigmoidal-like aggregation kinetics at the concentration examined (10 μM) whereby the lag-phase and subsequent fibril elongation begins at ∼1.5 h, reaching a plateau at ∼13 h (Figure 4A). In the presence of peptide **1**, no distinct change in aggregation kinetics was observed at a 1 : 1 molar ratio ($A\beta_{42}$ : inhibitor) compared with $A\beta_{42}$ alone (Figure 4A, blue), conferring only 2% inhibition (Figure 4B). At 1 : 10 and 1 : 20 molar ratios, a significant decrease in total fibril formation was observed, with plateaus at 10 h and 4 h, respectively with no change in lag-phase (i.e. primary nucleation) or elongation rate (Figure 4A). Subsequently, peptide **1** conferred 3% (1 : 1), 41% (1 : 10) and 70% (1 : 20)

Biochemical Journal (2020) 477 2039–2054
https://doi.org/10.1042/BCJ20200290

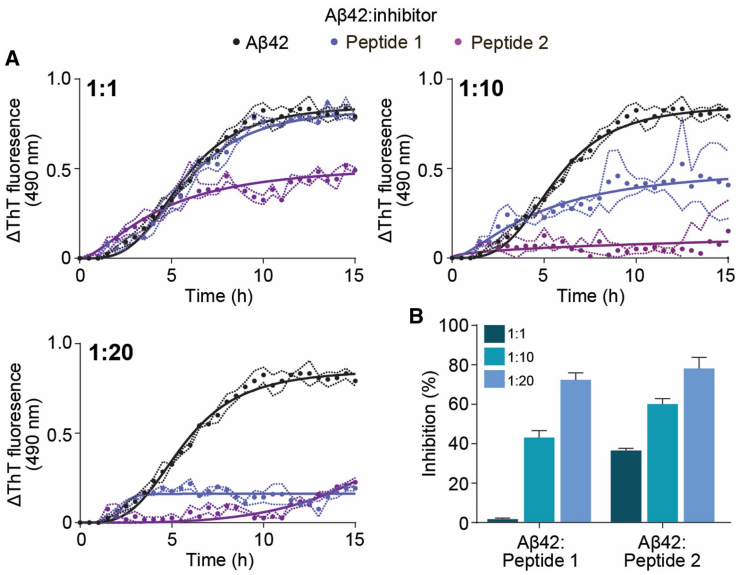


**Figure 4. Peptide 2 as a most effective inhibitor of $A\beta_{42}$ fibrilization.**

(**A**) ThT fluorescence assay monitoring fibril formation of $A\beta_{42}$ in the absence (10 μM, black) and presence of peptide inhibitors **1** (blue) and **2** (purple) at various molar ratios (ranging from 1 : 1 to 1 : 20, $A\beta_{42}$ : inhibitor). (**B**) The degree of inhibition of $A\beta_{42}$ fibril formation (calculated at the conclusion of the assay) induced by peptides **1** and **2** across the range of molar ratios examined. Data reported in A and B is presented as mean ± SEM ($n = 3$).

inhibition, whilst peptide **2** afforded 36% (1 : 1) and 60% (1 : 10) inhibition (Figure 4A,B). At a 1 : 20 molar ratio, peptide **2** drastically changes the aggregation kinetics of $A\beta_{42}$, extending the lag-phase to 7 h and slowing the rate of fibril elongation (Figure 4A, purple), resulting in 79% inhibition (Figure 4B). We propose that peptide **2** can interact with $A\beta_{42}$ monomers in order to prevent fibril formation, however further studies are needed to substantiate this notion, and these will be discussed in the following section. When combined with our fibril elongation assay data, the mechanism(s) of inhibition utilized by **1** and **2** are distinct as both predominantly interact with $A\beta_{42}$ fibrils, whilst peptide **2** also interacts with $A\beta_{42}$ monomers by inhibiting primary nucleation and subsequent fibril elongation.

## Peptide 2 induces conformational changes on aggregation-prone $A\beta_{42}$ monomers

Native ion-mobility mass spectrometry (IM-MS) and molecular modelling were used to determine whether peptides **1** and **2** modulate the conformation of aggregation-prone $A\beta_{42}$ monomers as an additional means of fibril inhibition (Figure 5). Native MS is a useful biophysical tool to probe the tertiary and quaternary structures, and dynamics of non-covalent protein-peptide assemblies (Figure 5A). When coupled to ion-mobility separation, the conformation of aggregation-prone assemblies can be visualized and assessed by observing the arrival time distribution (ATD) of individual protein species (e.g. monomers and dimers) during fibril formation (Figure 5B,C). In the absence of peptides **1** and **2**, $A\beta_{42}$ monomers undergo a disorder to order transition during incubation, as evidenced by the decrease in ATD (2.82 ms to 1.96 ms) after 2 h incubation, which is typical of fibril forming proteins [68] (Figure 5B,C). Upon addition of either peptides **1** or **2** prior to incubation, an ATD shift was observed. In the presence of peptide **1** (1.65 ms) and **2** (1.89 ms) this distribution (and hence monomer conformation) did not change further during aggregation (Figure 5B,C), which demonstrates that $A\beta_{42}$ monomers adopt a compact (i.e. more ordered) conformation upon immediate addition of inhibitor. The degree of heterogeneity within the monomer can be reported by the full-width half maximum (FWHM) (Figure 5D), where high FWHM values indicate monomers adopting more conformations across a broader ATD, and lower FWHM values indicate monomers adopting a comparatively restricted ensemble of conformations. The conformational heterogeneity of $A\beta_{42}$ monomers during incubation is reduced (1.88 to 1.34 ms) (Figure 5B,C). The immediate addition and incubation of **1** did not induce any change in conformational

*Biochemical Journal* (2020) **477** 2039–2054
https://doi.org/10.1042/BCJ20200290

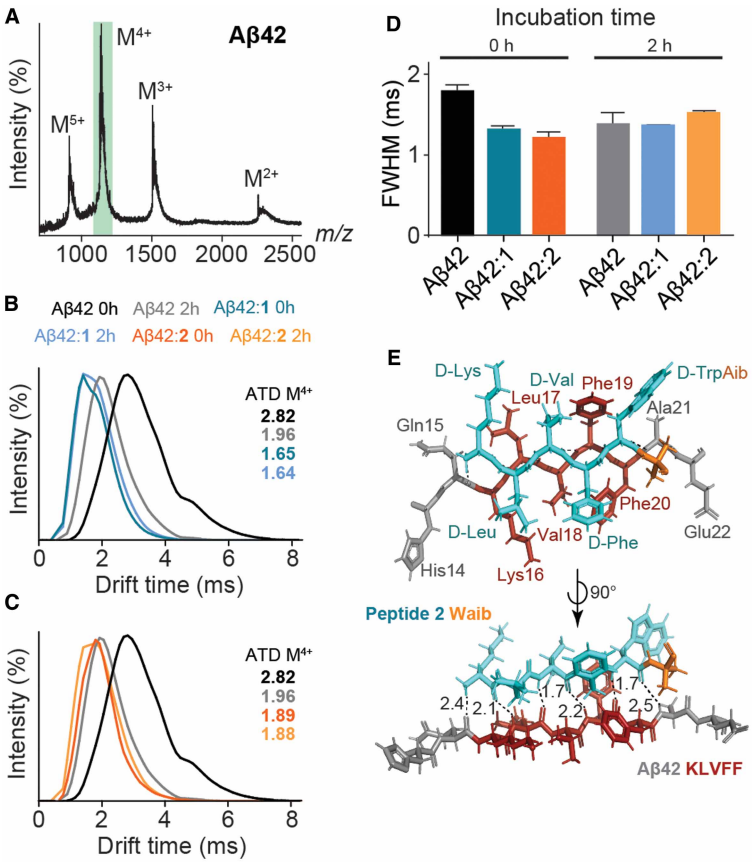


**Figure 5. Probing the interaction between peptides 1 and 2, and A$\beta_{42}$ monomers by native IM-MS and molecular modelling.**

(**A**) Native IM-MS of A$\beta_{42}$ (10 μM) in 200 mM ammonium acetate (pH 7.0) at 0 h with the monomer$^{4+}$ ($M^{4+}$; *m/z* 1128) being selected for ATD analysis (green box). (**B** and **C**) ATDs of A$\beta_{42}$ $M^{4+}$ during incubation with peptide **1** (**B**) and **2** (**C**) at a 1 : 10 molar ratio (A$\beta_{42}$ : peptide **1**/**2**) at low activation energies (10–20 V). A$\beta_{42}$ monomers in the absence of peptide **1** or **2** exhibit a disorder to order transition (black to grey) after 2 h incubation (37°C). The addition of peptides **1** (dark blue, 0 h; light blue, 2 h) or **2** (dark orange, 0 h; light orange, 2 h) immediately induces a conformational change of A$\beta_{42}$ monomers and persists during the initial stages of fibril formation (left panels). (**D**) FWHM time for A$\beta_{42}$ $M^{4+}$ ATDs in the absence and presence of **1** and **2** after 0 h and 2 h incubation (mean ± SD, $n = 3$). (**E**) Molecular modelling illustrates the interaction between a truncated segment of A$\beta_{42}$ (residues 14–22) and peptide **2** (light blue), mediated by strong H-bonding between residues klvfw of **2**, and KLVFF of A$\beta_{42}$, by virtue of their sequence homology (H-bond distances in Å, dashed lines).

heterogeneity of A$\beta_{42}$ monomers during incubation (1.26 to 1.30 ms) (Figure 5B, inset). However, upon immediate addition and subsequent incubation of A$\beta_{42}$ with **2**, we observed an increase in conformational heterogeneity (1.19 to 1.41 ms) (Figure 5D). This compaction and change in conformational heterogeneity of A$\beta_{42}$ monomers induces similar structural changes that are normally required for fibrilization, yet are unable to anneal on fibrils (i.e. fibril elongation), as has been previously suggested. [30]

In light of this ATD data, molecular modelling was employed to further probe the interaction between A$\beta_{42}$ monomers and peptide **2**. The modelling data demonstrates that peptide **2** is capable of forming six strong intermolecular H-bonds with a truncated segment of A$\beta_{42}$ (residues 14–22; HQKLVFFAE) (Figure 5E). The data also indicates that, like KLVFF, peptide **1** is prone to self-association via intermolecular H-bonding (Supplementary Figure S8A). Thus, there is competition with KLVFF and peptide **1**, between self-aggregation and interaction with A$\beta_{42}$. In contrast, peptide **2** does not self-aggregate (Supplementary Figure S8B) and preferentially binds to A$\beta_{42}$. We propose that peptide **2** induces conformational changes to A$\beta_{42}$ monomers through transient interactions, which is analogous to various fibrilization inhibitors such as molecular chaperones [76] and flavones. [77] The data shows that peptide **2** is capable of forming a strong H-bond network

*Biochemical Journal* (2020) **477** 2039–2054
https://doi.org/10.1042/BCJ20200290

specific to residues 16–20 of $A\beta_{42}$. This 'in-register' parallel β-sheet architecture is found in the hydrophobic central core region of Aβ [78] and is common to most other pathological human amyloids. [79] This arrangement, with the all D-peptide forming intermolecular hydrogen bonds with the all L-$A\beta_{42}$ peptide, positions the side chains of the adjacent peptides opposite to one another, which would help alleviate charge repulsion between lysine residues. Supplementary Figure S9 shows the model of peptide **2** from above, with residues 1–5 comprising a β-strand structure, with the exception of the Aib residue. Each backbone carbonyl and amide hydrogen of amino acids 1–5 are positioned as a β-strand, whereas those associated with the Aib residue adopt a different orientation, which is not conducive to intermolecular hydrogen bonding to $A\beta_{42}$ from above or below. We have previously shown the geminally disubstituted Aib residue to reduce backbone flexibility within a peptide. [80] Collectively, our results demonstrate that peptide **2** interacts with both monomeric and fibrillar $A\beta_{42}$ to inhibit fibril formation and elongation. This interaction is sequence-specific, with the C-terminal Aib β-breakage moiety of **2** preventing further intermolecular hydrogen bonding, thus impeding the self-assembly process.

## Peptide 2 significantly reduces hydrophobicity of $A\beta_{42}$ fibrils

To further understand the mechanism(s) by which **1** and **2** interact with $A\beta_{42}$, we investigated whether these peptides could reduce the exposed hydrophobicity of $A\beta_{42}$ fibrils (Figure 6A,B). Fibrils were labelled with Nile red (10 μM) in the absence and presence of peptides **1** and **2** at the molar ratios tested in the ThT fluorescence assays (see Materials and Methods section for details). No shift in the emission wavelength was observed in the absence or presence of peptides **1** and **2** (Figure 6A,B). Upon treatment with either peptide, there was an observable concentration-dependent decrease in Nile red fluorescence, with peptide **2** inducing a considerably greater decrease in fluorescence intensity compared with peptide **1** at a 1 : 20 molar ratio ($A\beta_{42}$ : inhibitor) (Figure 6A,B). This indicates that peptide **2** decreases the surface hydrophobicity of $A\beta_{42}$ fibrils, potentially reducing their toxicity.

## Peptide 2 significantly reduces cytotoxicity of $A\beta_{42}$ fibrils

The cytotoxic effects of $A\beta_{42}$ aggregation on various cell types are well known, [81] and here we investigate the ability of these peptide-based inhibitors to decrease cytotoxicity in the presence of $A\beta_{42}$ fibrils using an MTT cell viability assay (see Materials and Methods section for details). Firstly, the presence of inhibitors to specifically exert cytotoxic effects on cells was examined (Figure 7). Cells treated with both $A\beta_{42}$ and inhibitors were analyzed at a 1 : 2 molar ratio ($A\beta_{42}$ : inhibitor). Across all compounds tested, there was no drastic change in cell viability in the absence of $A\beta_{42,}$ indicating that the inhibitors (and controls) alone do not affect cell viability. Upon addition of exogenous $A\beta_{42}$ fibrils to murine neuroblastoma Neuro-2a cells, a substantial decrease in cell viability was observed (~56% decrease, Figure 7A,B). The addition of either wAib or KLVFF in the presence of $A\beta_{42}$ fibrils does not significantly increase cell viability compared with cells incubated with $A\beta_{42}$ alone (Figure 7A). However, the addition of peptides **1** and **2** significantly increases cell viability to ~90% and ~99%, respectively, compared with $A\beta_{42}$ alone (Figure 7A). Overall, the data indicates that peptides **1** and **2** are both biocompatible, and reduce $A\beta_{42}$ fibril-induced toxicity at the cellular level. Most notably, peptide **2** incubated with $A\beta_{42,}$ drastically restores cell viability.

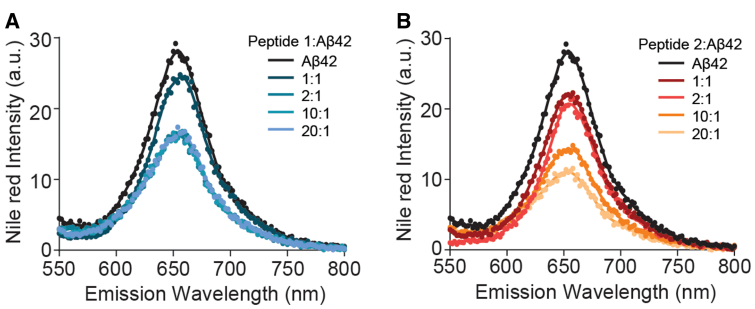


**Figure 6. Peptide 2 significantly reduces hydrophobicity of $A\beta_{42}$ fibrils.**

(**A** and **B**) Nile red emission fluorescence of $A\beta_{42}$ fibrils (10 μM) in the absence and presence of peptides **1** (**A**) and **2** (**B**) at various molar ratios (1 : 1 to 20 : 1, peptide : $A\beta_{42}$).

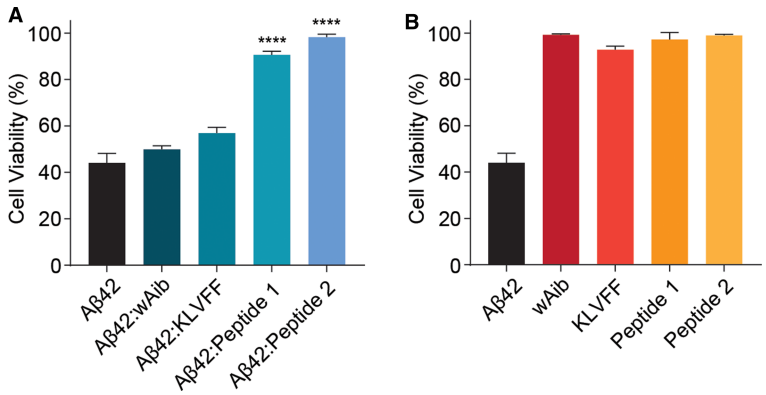


**Figure 7. Peptide 2 significantly restores cell viability upon addition of $A\beta_{42}$ fibrils.**

(**A** and **B**) Neuro-2a cells were treated with various inhibitors in the presence (**A**) and absence (**B**) of pre-formed $A\beta_{42}$ fibrils (50 μM). Cells treated with both $A\beta_{42}$ and inhibitors were examined at a 1 : 2 molar ratio ($A\beta_{42}$ : inhibitor). Cells were incubated for 24 h and cell viability was measured upon addition of MTT (0.5 mg/ml). Data reported is presented as mean ± SEM ($n = 3$) (** $P < 0.01$, **** $P < 0.0001$).

In summary, the aggregation of $A\beta_{42}$ monomers to potentially neurotoxic oligomers and fibrils is believed to be responsible for the onset of AD, with the first step in this process being a conformational change to a β-sheet geometry. Inhibitors designed expressly for $A\beta_{42}$ aggregation require high specificity, hence the design and synthesis of peptide **2** was based on the β-strand-containing KLVFF region of the amyloid peptide, together with an Aib β-sheet disruption element. This is the first study of its type to successfully exploit the synergy between a recognition and disruption component incorporated into a peptide comprising D-amino acids, for the specific inhibition of $A\beta_{42}$ aggregation. NMR and IR data, together with molecular modelling, confirm the presence of a β-strand conformation throughout the inhibitor, with the exception of the Aib 'β-breaker' moiety. Experimental data show that peptide **2** prevents fibril formation, specifically towards $A\beta_{42}$, and significantly reduces the rate of fibril elongation, such that a two-fold excess essentially halts fibril elongation altogether. This peptide-based inhibitor preferentially interacts with $A\beta_{42}$ fibrils by slowing elongation, likely interacting with the ends of fibrils, to prevent further fibril formation. Aggregation assays, native IM-MS and molecular modelling were used to demonstrate that peptide **2** is also capable of interacting with $A\beta_{42}$ monomers to prevent oligomerization and inhibit aggregation. These results shed light on the binding mechanism and further underline the significance of the β-strand structure, and particular D-amino acid sequence, for specificity towards $A\beta_{42}$. Cell viability assays demonstrate that when incubated with $A\beta_{42}$ in a 2:1 molar ratio, peptide **2** exhibits essentially no cytotoxic effect whatsoever. Moreover, an effective inhibitor should not self-aggregate and, unlike the KLVFF peptide fragment, **2** fulfils this requirement. Collectively, our results show peptide **2** to be a potent inhibitor of $A\beta_{42}$ monomers, oligomers and fibrils, and thus offers considerable promise for further development as a drug candidate in the treatment of AD. We set out to exploit the synergy between the recognition and disruption components incorporated into the peptide-based inhibitor, and found that the sum is greater than its parts. The synergistic rationale employed in this study could potentially be applied to enhance therapeutic efficacy for fibril forming proteins that are associated with other neurodegenerative diseases.

## Competing Interests

The authors declare that there are no competing interests associated with the manuscript.

## Funding

The authors acknowledge the Australian Research Council (ARC) Discovery Project (DP180101581) and the Centre of Excellence for Nanoscale BioPhotonics (CNBP) for financial support. We also acknowledge funding from the Australian Research Council (ARC) Discovery Project (DP170102033) and National Health and Medical Research Council (NHMRC) (44113151).

*Biochemical Journal* (2020) **477** 2039–2054
https://doi.org/10.1042/BCJ20200290

## Open Access

Open access for this article was enabled by the participation of University of Adelaide in an all-inclusive *Read & Publish* pilot with Portland Press and the Biochemical Society under a transformative agreement with CAUL.

## Author Contributions

J.R.H. designed the research, synthesized the peptides, and prepared the manuscript. B.J. designed the research, conducted assays and prepared the manuscript. K.L.W. conducted assays. J.Y. undertook computational studies. T.L.P. and A.D.A. contributed to the manuscript.

## Acknowledgements

We thank the Australian National Fabrication Facility (ANFF) for providing the analytical facilities used in this work, and Flinders Analytical (Flinders University, Australia) for access and support to IM-MS instrumentation. We also thank Dr. Lisa O'Donovan and Adelaide Microscopy (both University of Adelaide) for TEM technical assistance, and Prof. John A. Carver (Australian National University) for his input. Computational aspects of this work were supported by an award under the National Computational Merit Allocation Scheme for JY on the National Computing Infrastructure (NCI) National Facility at the Australian National University.

## Abbreviations

AD, Alzheimer's disease; ATD, arrival time distribution; BBB, blood brain barrier; FWHM, full-width half maximum; IM-MS, ion-mobility mass spectrometry; SPPS, solid phase peptide synthesis; TEM, transmission electron microscopy; WT, wild type.

# References

1 van Groen, T., Schemmert, S., Brener, O., Gremer, L., Ziehm, T., Tusche, M. et al. (2017) The Aβ oligomer eliminating D-enantiomeric peptide RD2 improves cognition without changing plaque pathology. *Sci. Rep.* **7**, 16275 https://doi.org/10.1038/s41598-017-16565-1

2 Frydman-Marom, A., Convertino, M., Pellarin, R., Lampel, A., Shaltiel-Karyo, R., Segal, D. et al. (2011) Structural basis for inhibiting β-amyloid oligomerization by a non-coded β-breaker-substituted endomorphin analogue. *ACS Chem. Biol.* **6**, 1265–1276 https://doi.org/10.1021/cb200103h

3 Warner, C.J.A., Dutta, S., Foley, A.R. and Raskatov, J.A. (2016) Introduction of d-glutamate at a critical residue of Aβ42 stabilizes a prefibrillary aggregate with enhanced toxicity. *Chemistry* **22**, 11967–11970 https://doi.org/10.1002/chem.201601763

4 Cacabelos, R. (2018) Have there been improvements in Alzheimer's disease drug discovery over the past 5 years? *Expert Opin. Drug Discov.* **13**, 523–538 https://doi.org/10.1080/17460441.2018.1457645

5 Nie, Q., Du, X.G. and Geng, M.Y. (2011) Small molecule inhibitors of amyloid β peptide aggregation as a potential therapeutic strategy for Alzheimers disease. *Acta Pharmacol. Sin.* **32**, 545 https://doi.org/10.1038/aps.2011.14

6 Kasim, J.K., Kavianinia, I., Harris, P.W.R. and Brimble, M.A. (2019) Three decades of amyloid beta synthesis: challenges and advances. *Front Chem* **7**, 472 https://doi.org/10.3389/fchem.2019.00472

7 Yan, R. and Vassar, R. (2014) Targeting the β secretase BACE1 for Alzheimer's disease therapy. *Lancet Neurol.* **13**, 319–329 https://doi.org/10.1016/S1474-4422(13)70276-X

8 Barrera Guisasola, E.E., Andujar, S.A., Hubin, E., Broersen, K., Kraan, I.M., Méndez, L. et al. (2015) New mimetic peptides inhibitors of Aβ aggregation. Molecular guidance for rational drug design. *Eur. J. Med. Chem.* **95**, 136–152 https://doi.org/10.1016/j.ejmech.2015.03.042

9 Lin, Y.-S., Bowman, G.R., Beauchamp, K.A. and Pande, V.S. (2012) Investigating how peptide length and a pathogenic mutation modify the structural ensemble of amyloid beta monomer. *Biophys. J.* **102**, 315–324 https://doi.org/10.1016/j.bpj.2011.12.002

10 Lee, H.J., Korshavn, K.J., Nam, Y., Kang, J., Paul, T.J., Kerr, R.A. et al. (2017) Structural and mechanistic insights into development of chemical tools to control individual and inter-related pathological features in Alzheimer's disease. *Chemistry* **23**, 2706–2715 https://doi.org/10.1002/chem.201605401

11 Kaffy, J., Brinet, D., Soulier, J.-L., Correia, I., Tonali, N., Fera, K.F. et al. (2016) Designed glycopeptidomimetics disrupt protein–Protein interactions mediating amyloid β-peptide aggregation and restore neuroblastoma cell viability. *J. Med. Chem.* **59**, 2025–2040 https://doi.org/10.1021/acs.jmedchem.5b01629

12 Goyal, D., Shuaib, S., Mann, S. and Goyal, B. (2017) Rationally designed peptides and peptidomimetics as inhibitors of amyloid-β (Aβ) aggregation: potential therapeutics of Alzheimer's disease. *ACS Comb. Sci.* **19**, 55–80 https://doi.org/10.1021/acscombsci.6b00116

13 Coimbra, J.R.M., Marques, D.F.F., Baptista, S.J., Pereira, C.M.F., Moreira, P.I., Dinis, T.C.P. et al. (2018) Highlights in BACE1 inhibitors for Alzheimer's disease treatment. *Front. Chem.* **6**, 178 https://doi.org/10.3389/fchem.2018.00178

14 Bisceglia, F., Natalello, A., Serafini, M.M., Colombo, R., Verga, L., Lanni, C. et al. (2018) An integrated strategy to correlate aggregation state, structure and toxicity of Aß 1–42 oligomers. *Talanta* **188**, 17–26 https://doi.org/10.1016/j.talanta.2018.05.062

15 Oliveri, V., Zimbone, S., Giuffrida, M.L., Bellia, F., Tomasello, M.F. and Vecchio, G. (2018) Porphyrin cyclodextrin conjugates modulate amyloid beta peptide aggregation and cytotoxicity. *Chemistry* **24**, 6349–6353 https://doi.org/10.1002/chem.201800807

16 Parsons, C.G. and Rammes, G. (2017) Preclinical to phase II amyloid beta (Aβ) peptide modulators under investigation for Alzheimer's disease. *Expert Opin. Invest. Drugs* **26**, 579–592 https://doi.org/10.1080/13543784.2017.1313832

17 Oren, O., Banerjee, V., Taube, R. and Papo, N. (2018) An Aβ42 variant that inhibits intra- and extracellular amyloid aggregation and enhances cell viability. *Biochem. J.* **475**, 3087–3103 https://doi.org/10.1042/BCJ20180247

18 Cardoso, M.H., Cândido, E.S., Oshiro, K.G.N., Rezende, S.B. and Franco, O.L. (2018) Peptides containing d-amino acids and retro-inverso peptides: General applications and special focus on antimicrobial peptides. In *Peptide Applications in Biomedicine, Biotechnology and Bioengineering* (Koutsopoulos, S., ed.), pp. 131–155, Woodhead Publishing

19 Siddiqi, M.K., Alam, P., Iqbal, T., Majid, N., Malik, S., Nusrat, S. et al. (2018) Elucidating the inhibitory potential of designed peptides against amyloid fibrillation and amyloid associated cytotoxicity. *Front. Chem.* **6**, 311 https://doi.org/10.3389/fchem.2018.00311
20 Yeoh, Y.Q., Yu, J., Polyak, S.W., Horsley, J.R. and Abell, A.D. (2018) Photopharmacological control of cyclic antimicrobial peptides. *ChemBioChem* **19**, 2591–2597 https://doi.org/10.1002/cbic.201800618
21 Lowe, T.L., Strzelec, A., Kiessling, L.L. and Murphy, R.M. (2001) Structure–function relationships for inhibitors of β-amyloid toxicity containing the recognition sequence KLVFF. *Biochemistry* **40**, 7882–7889 https://doi.org/10.1021/bi002734u
22 Tjernberg, L.O., Näslund, J., Lindqvist, F., Johansson, J., Karlström, A.R., Thyberg, J. et al. (1996) Arrest of beta-Amyloid fibril formation by a pentapeptide ligand. *J. Biol Chem.* **271**, 8545–8548 https://doi.org/10.1074/jbc.271.15.8545
23 Arai, T., Sasaki, D., Araya, T., Sato, T., Sohma, Y. and Kanai, M. (2014) A cyclic KLVFF-Derived peptide aggregation inhibitor induces the formation of less-toxic off-pathway amyloid-β oligomers. *ChemBioChem* **15**, 2577–2583 https://doi.org/10.1002/cbic.201402430
24 Tran, L. and Ha-Duong, T. (2015) Exploring the Alzheimer amyloid-β peptide conformational ensemble: A review of molecular dynamics approaches. *Peptides* **69**, 86–91 https://doi.org/10.1016/j.peptides.2015.04.009
25 Breydo, L., Kurouski, D., Rasool, S., Milton, S., Wu, J.W., Uversky, V.N. et al. (2016) Structural differences between amyloid beta oligomers. *Biochem. Biophys. Res. Commun.* **477**, 700–705 https://doi.org/10.1016/j.bbrc.2016.06.122
26 Matsubara, T., Yasumori, H., Ito, K., Shimoaka, T., Hasegawa, T. and Sato, T. (2018) Amyloid-β fibrils assembled on ganglioside-enriched membranes contain both parallel β-sheets and turns. *J. Biol. Chem.* **293**, 14146–14154 https://doi.org/10.1074/jbc.RA118.002787
27 Cheng, P.-N., Liu, C., Zhao, M., Eisenberg, D. and Nowick, J.S. (2012) Amyloid β-sheet mimics that antagonize protein aggregation and reduce amyloid toxicity. *Nat. Chem.* **4**, 927 https://doi.org/10.1038/nchem.1433
28 Tjernberg, L.O., Lilliehöök, C., Callaway, D.J.E., Näslund, J., Hahne, S., Thyberg, J. et al. (1997) Controlling amyloid β-peptide fibril formation with protease-stable ligands. *J. Biol. Chem.* **272**, 12601–12605 https://doi.org/10.1074/jbc.272.19.12601
29 Zhang-Haagen, B., Biehl, R., Nagel-Steger, L., Radulescu, A., Richter, D. and Willbold, D. (2016) Monomeric amyloid beta peptide in hexafluoroisopropanol detected by small angle neutron scattering. *PLoS ONE.* **11**, e0150267 https://doi.org/10.1371/journal.pone.0150267
30 Colvin, M.T., Silvers, R., Ni, Q.Z., Can, T.V., Sergeyev, I., Rosay, M. et al. (2016) Atomic resolution structure of monomorphic Aβ42 amyloid fibrils. *J. Am. Chem. Soc.* **138**, 9663–9674 https://doi.org/10.1021/jacs.6b05129
31 Wälti, M.A., Ravotti, F., Arai, H., Glabe, C.G., Wall, J.S., Böckmann, A. et al. (2016) Atomic-resolution structure of a disease-relevant Aβ(1–42) amyloid fibril. *Proc. Natl Acad. Sci. U.S.A.* **113**, E4976–E4984 https://doi.org/10.1073/pnas.1600749113
32 Gremer, L., Schölzel, D., Schenk, C., Reinartz, E., Labahn, J., Ravelli, R.B.G. et al. (2017) Fibril structure of amyloid-β(1–42) by cryo–electron microscopy. *Science* **358**, 116–119 https://doi.org/10.1126/science.aao2825
33 Eisenberg, D.S. and Sawaya, M.R. (2017) Structural studies of amyloid proteins at the molecular level. *Annu. Rev. Biochem.* **86**, 69–95 https://doi.org/10.1146/annurev-biochem-061516-045104
34 Xiao, Y., Ma, B., McElheny, D., Parthasarathy, S., Long, F., Hoshi, M. et al. (2015) Aβ(1–42) fibril structure illuminates self-recognition and replication of amyloid in Alzheimer's disease. *Nat. Struct. Mol. Biol.* **22**, 499 https://doi.org/10.1038/nsmb.2991
35 Eisenberg, D.S. and Sawaya, M.R. (2016) Implications for Alzheimer's disease of an atomic resolution structure of amyloid-β(1–42) fibrils. *Proc. Natl Acad. Sci. U.S.A.* **113**, 9398–9400 https://doi.org/10.1073/pnas.1610806113
36 Chafekar, S.M., Malda, H., Merkx, M., Meijer, E.W., Viertl, D., Lashuel, H.A. et al. (2007) Branched KLVFF tetramers strongly potentiate inhibition of β-amyloid aggregation. *ChemBioChem* **8**, 1857–1864 https://doi.org/10.1002/cbic.200700338
37 Austen, B.M., Paleologou, K.E., Ali, S.A.E., Qureshi, M.M., Allsop, D. and El-Agnaf, O.M.A. (2008) Designing peptide inhibitors for oligomerization and toxicity of Alzheimer's β-amyloid peptide. *Biochemistry* **47**, 1984–1992 https://doi.org/10.1021/bi701415b
38 Kino, R., Araya, T., Arai, T., Sohma, Y. and Kanai, M. (2015) Covalent modifier-type aggregation inhibitor of amyloid-β based on a cyclo-KLVFF motif. *Bioorg. Med. Chem. Lett.* **25**, 2972–2975 https://doi.org/10.1016/j.bmcl.2015.05.027
39 Gordon, D.J., Sciarretta, K.L. and Meredith, S.C. (2001) Inhibition of β-amyloid(40) fibrillogenesis and disassembly of β-amyloid(40) fibrils by short β-amyloid congeners containing N-methyl amino acids at alternate residues. *Biochemistry* **40**, 8237–8245 https://doi.org/10.1021/bi002416v
40 Matharu, B., El-Agnaf, O., Razvi, A. and Austen, B.M. (2010) Development of retro-inverso peptides as anti-aggregation drugs for β-amyloid in Alzheimer's disease. *Peptides* **31**, 1866–1872 https://doi.org/10.1016/j.peptides.2010.06.033
41 Kokkoni, N., Stott, K., Amijee, H., Mason, J.M. and Doig, A.J. (2006) N-Methylated peptide inhibitors of β-amyloid aggregation and toxicity. optimization of the inhibitor structure. *Biochemistry* **45**, 9906–9918 https://doi.org/10.1021/bi060837s
42 Rajasekhar, K., Suresh, S.N., Manjithaya, R. and Govindaraju, T. (2015) Rationally designed peptidomimetic modulators of Aβ toxicity in Alzheimer's disease. *Sci. Rep.* **5**, 8139 https://doi.org/10.1038/srep08139
43 Hamley, I.W. (2007) Peptide fibrillization. *Angew. Chem. Int. Ed. Engl.* **46**, 8128–8147 https://doi.org/10.1002/anie.200700861
44 Chalifour, R.J., McLaughlin, R.W., Lavoie, L., Morissette, C., Tremblay, N., Boulé, M. et al. (2003) Stereoselective interactions of peptide inhibitors with the β-amyloid peptide. *J. Biol. Chem.* **278**, 34874–34881 https://doi.org/10.1074/jbc.M212694200
45 Arai, T., Araya, T., Sasaki, D., Taniguchi, A., Sato, T., Sohma, Y. et al. (2014) Rational design and identification of a non-peptidic aggregation inhibitor of amyloid-β based on a pharmacophore motif obtained from cyclo[-Lys-Leu-Val-Phe-Phe-]. *Angew. Chem. Int. Ed. Engl.* **53**, 8236–8239 https://doi.org/10.1002/anie.201405109
46 Jagota, S. and Rajadas, J. (2013) Synthesis of d-amino acid peptides and their effect on beta-amyloid aggregation and toxicity in transgenic caenorhabditis elegans. *Med. Chem. Res.* **22**, 3991–4000 https://doi.org/10.1007/s00044-012-0386-2
47 Dammers, C., Yolcu, D., Kukuk, L., Willbold, D., Pickhardt, M., Mandelkow, E. et al. (2016) Selection and characterization of tau binding D-Enantiomeric peptides with potential for therapy of Alzheimer disease. *PLoS ONE.* **11**, e0167432 https://doi.org/10.1371/journal.pone.0167432
48 Leithold, L.H.E., Jiang, N., Post, J., Ziehm, T., Schartmann, E., Kutzsche, J. et al. (2016) Pharmacokinetic properties of a novel d-peptide developed to be therapeutically active against toxic β-amyloid oligomers. *Pharm. Res.* **33**, 328–336 https://doi.org/10.1007/s11095-015-1791-2
49 Spanopoulou, A., Heidrich, L., Chen, H.-R., Frost, C., Hrle, D., Malideli, E. et al. (2018) Designed macrocyclic peptides as nanomolar amyloid inhibitors based on minimal recognition elements. *Angew. Chem. Int. Ed. Engl.* **57**, 14503–14508 https://doi.org/10.1002/anie.201802979
50 Ghanta, J., Shen, C.-L., Kiessling, L.L. and Murphy, R.M. (1996) A strategy for designing inhibitors of β-amyloid toxicity. *J. Biol. Chem.* **271**, 29525–29528 https://doi.org/10.1074/jbc.271.47.29525

*Biochemical Journal* (2020) **477** 2039–2054
https://doi.org/10.1042/BCJ20200290


51 Etienne, M.A., Aucoin, J.P., Fu, Y., McCarley, R.L. and Hammer, R.P. (2006) Stoichiometric inhibition of amyloid β-protein aggregation with peptides containing alternating α,α-disubstituted amino acids. *J. Am. Chem. Soc.* **128**, 3522–3523 https://doi.org/10.1021/ja0600678

52 Sciarretta, K.L., Gordon, D.J. and Meredith, S.C. (2006) Peptide-based inhibitors of amyloid assembly. *Methods Enzymol.* **413**, 273–312 https://doi.org/10.1016/S0076-6879(06)13015-3

53 Soto, C., Kindy, M.S., Baumann, M. and Frangione, B. (1996) Inhibition of Alzheimer's amyloidosis by peptides that prevent β-Sheet conformation. *Biochem. Biophys. Res. Commun.* **226**, 672–680 https://doi.org/10.1006/bbrc.1996.1413

54 Botz, A., Gasparik, V., Devillers, E., Hoffmann, A.R.F., Caillon, L., Chelain, E. et al. (2015) (R)-α-trifluoromethylalanine containing short peptide in the inhibition of amyloid peptide fibrillation. *Peptide Sci.* **104**, 601–610 https://doi.org/10.1002/bip.22670

55 Gilead, S. and Gazit, E. (2004) Inhibition of amyloid fibril formation by peptide analogues modified with α-aminoisobutyric acid. *Angew. Chem. Int. Ed. Engl.* **116**, 4133–4136 https://doi.org/10.1002/ange.200353565

56 Frydman-Marom, A., Rechter, M., Shefler, I., Bram, Y., Shalev, D.E. and Gazit, E. (2009) Cognitive-Performance recovery of Alzheimer's disease model mice by modulation of early soluble amyloidal assemblies. *Angew. Chem. Int. Ed. Engl.* **121**, 2015–2020 https://doi.org/10.1002/ange.200802123

57 Formaggio, F., Bettio, A., Moretto, V., Crisma, M., Toniolo, C. and Broxterman, Q.B. (2003) Disruption of the β-sheet structure of a protected pentapeptide, related to the β-amyloid sequence 17–21, induced by a single, helicogenic Cα-tetrasubstituted α-amino acid. *J. Pept. Sci.* **9**, 461–466 https://doi.org/10.1002/psc.503

58 Parsons, C.G., Ruitenberg, M., Freitag, C.E., Sroka-Saidi, K., Russ, H. and Rammes, G. (2015) MRZ-99030 – A novel modulator of Aβ aggregation: I – mechanism of action (MoA) underlying the potential neuroprotective treatment of Alzheimer's disease, glaucoma and age-related macular degeneration (AMD). *Neuropharmacology* **92**, 158–169 https://doi.org/10.1016/j.neuropharm.2014.12.038

59 Frydman-Marom, A., Shaltiel-Karyo, R., Moshe, S. and Gazit, E. (2011) The generic amyloid formation inhibition effect of a designed small aromatic β-breaking peptide. *Amyloid* **18**, 119–127 https://doi.org/10.3109/13506129.2011.582902

60 Bett, C.K., Serem, W.K., Fontenot, K.R., Hammer, R.P. and Garno, J.C. (2010) Effects of peptides derived from terminal modifications of the Aβ central hydrophobic core on Aβ fibrillization. *ACS Chem. Neurosci.* **1**, 661–678 https://doi.org/10.1021/cn900019r

61 Zhang, L., Yagnik, G., Peng, Y., Wang, J., Xu, H.H., Hao, Y. et al. (2013) Kinetic studies of inhibition of the amyloid beta (1-42) aggregation using a ferrocene-tagged β-sheet breaker peptide. *Anal. Biochem.* **434**, 292–299 https://doi.org/10.1016/j.ab.2012.11.025

62 Barz, B. and Strodel, B. (2016) Understanding amyloid-β oligomerization at the molecular level: the role of the fibril surface. *Chemistry* **22**, 8768–8772 https://doi.org/10.1002/chem.201601701

63 Valiev, M., Bylaska, E.J., Govind, N., Kowalski, K., Straatsma, T.P., van Dam, H.J.J. et al. (2010) NWChem: a comprehensive and scalable open-source solution for large scale molecular simulations. *Comput. Phys. Commun.* **181**, 1477 https://doi.org/10.1016/j.cpc.2010.04.018

64 Pettersen, E.F., Goddard, T.D., Huang, C.C., Couch, G.S., Greenblatt, D.M., Meng, E.C. et al. (2004) UCSF chimera—A visualization system for exploratory research and analysis. *J. Comput. Chem.* **25**, 1605–1612 https://doi.org/10.1002/jcc.20084

65 Ryan, T.M., Caine, J., Mertens, H.D.T., Kirby, N., Nigro, J., Breheney, K. et al. (2013) Ammonium hydroxide treatment of Aβ produces an aggregate free solution suitable for biophysical and cell culture characterization. *PeerJ* **1**, e73–e73 https://doi.org/10.7717/peerj.73

66 Ecroyd, H. and Carver, J.A. (2008) The effect of small molecules in modulating the chaperone activity of αB-crystallin against ordered and disordered protein aggregation. *FEBS J.* **275**, 935–947 https://doi.org/10.1111/j.1742-4658.2008.06257.x

67 Buell, A.K., Galvagnion, C., Gaspar, R., Sparr, E., Vendruscolo, M., Knowles, T.P.J. et al. (2014) Solution conditions determine the relative importance of nucleation and growth processes in α-synuclein aggregation. *Proc. Natl Acad. Sci. U.S.A.* **111**, 7671–7676 https://doi.org/10.1073/pnas.1315346111

68 Liu, Y., Jovcevski, B. and Pukala, T.L. (2019) C-Phycocyanin from spirulina inhibits α-synuclein and amyloid-β fibril formation but not amorphous aggregation. *J. Nat. Prod.* **82**, 66–73 https://doi.org/10.1021/acs.jnatprod.8b00610

69 Jiang, N., Frenzel, D., Schartmann, E., van Groen, T., Kadish, I., Shah, N.J. et al. (2016) Blood-brain barrier penetration of an Aβ-targeted, arginine-rich, d-enantiomeric peptide. *Biochim. Biophys. Acta* **1858**, 2717–2724 https://doi.org/10.1016/j.bbamem.2016.07.002

70 Fernando, S.R.L., Kozlov, G.V. and Ogawa, M.Y. (1998) Distance dependence of electron transfer along artificial beta-strands at 298 and 77K. *Inorg. Chem.* **37**, 1900–1905 https://doi.org/10.1021/ic970369y

71 Zhuang, W., Hayashi, T. and Mukamel, S. (2009) Coherent multidimensional vibrational spectroscopy of biomolecules: Concepts, simulations, and challenges. *Angew. Chem. Int. Ed.Engl.* **48**, 3750–3781 https://doi.org/10.1002/anie.200802644

72 Gillespie, P., Cicariello, J. and Olson, G.L. (1997) Conformational analysis of dipeptide mimetics. *Pept. Sci.* **43**, 191–217 https://doi.org/10.1002/(SICI)1097-0282(1997)43:3<191::AID-BIP2>3.0.CO;2-Q

73 Hasegawa, K., Yamaguchi, I., Omata, S., Gejyo, F. and Naiki, H. (1999) Interaction between Aβ(1−42) and Aβ(1−40) in Alzheimer's β-Amyloid fibril formation in vitro. *Biochemistry* **38**, 15514–15521 https://doi.org/10.1021/bi991161m

74 Li, B., Ge, P., Murray, K.A., Sheth, P., Zhang, M., Nair, G. et al. (2018) Cryo-EM of full-length α-synuclein reveals fibril polymorphs with a common structural kernel. *Nat. Commun.* **9**, 3609 https://doi.org/10.1038/s41467-018-05971-2

75 Cater, J.H., Kumita, J.R., Zeineddine Abdallah, R., Zhao, G., Bernardo-Gancedo, A., Henry, A. et al. (2019) Human pregnancy zone protein stabilizes misfolded proteins including preeclampsia- and Alzheimer's-associated amyloid beta peptide. *Proc. Natl Acad. Sci. U.S.A.* **116**, 6101 https://doi.org/10.1073/pnas.1817298116

76 Cox, D., Selig, E., Griffin, M.D.W., Carver, J.A. and Ecroyd, H. (2016) Small heat-shock proteins prevent α-synuclein aggregation via transient interactions and their efficacy Is affected by the rate of aggregation. *J. Biol. Chem.* **291**, 22618–22629 https://doi.org/10.1074/jbc.M116.739250

77 Das, S., Pukala, T.L. and Smid, S.D. (2018) Exploring the structural diversity in inhibitors of α-synuclein amyloidogenic folding, aggregation, and neurotoxicity. *Front. Chem.* **6**, 181 https://doi.org/10.3389/fchem.2018.00181

78 Benzinger, T.L.S., Gregory, D.M., Burkoth, T.S., Miller-Auer, H., Lynn, D.G., Botto, R.E. et al. (1998) Propagating structure of Alzheimer's β-amyloid (10–35) is parallel β-sheet with residues in exact register. *Proc. Natl Acad. Sci. U.S.A.* **95**, 13407–13412 https://doi.org/10.1073/pnas.95.23.13407

79 Gorkovskiy, A., Thurber, K.R., Tycko, R. and Wickner, R.B. (2014) Locating folds of the in-register parallel β-sheet of the Sup35p prion domain infectious amyloid. *Proc. Natl Acad. Sci. U.S.A.* **111**, E4615–E4622 https://doi.org/10.1073/pnas.1417974111

80 Yu, J., Horsley, J.R., Moore, K.E., Shapter, J.G. and Abell, A.D. (2014) The effect of a macrocyclic constraint on electron transfer in helical peptides: A step towards tunable molecular wires. *Chem. Commun.* **50**, 1652 https://doi.org/10.1039/c3cc47885h

81 Ziehm, T., Brener, O., van Groen, T., Kadish, I., Frenzel, D., Tusche, M. et al. (2016) Increase of positive Net charge and conformational rigidity enhances the efficacy of d-enantiomeric peptides designed to eliminate cytotoxic Aβ species. *ACS Chem. Neurosci.* **7**, 1088–1096 https://doi.org/10.1021/acschemneuro.6b00047